PORTIONS

OF THIS

DOCUMENT

ARE

ILLEGIBLE

BLANK PAGE

LA-UR-75-1804

TITLE: CRACK IDENTIFICATION AND CHARACTERIZATION
IN LONG WAVELENGTH ELASTIC WAVE SCATTERING

AUTHOR(S):   J. E. Gubernatis
and
E. Domany

SUBMITTED TO: First International Symposium
on Ultrasonic Materials
Characterization, June 7-9, 1978
NBS, Gaithersburg, Maryland

los alamos
scientific laboratory
of the University of California
LOS ALAMOS NEW MEXICO 87545

CRACK IDENTIFICATION AND CHARACTERIZATION

IN LONG WAVELENGTH ELASTIC WAVE SCATTERING

by

J. E. Gubernatis[*]
Theoretical Division, University of California
Los Alamos Scientific Laboratory
Los Alamos, New Mexico 87545

and

E. Domany
Department of Physics, University of Washington
Seattle, Washington 98195

ABSTRACT

We discuss apparent characteristic features of Rayleigh scattering of elastic waves from cracks. Interpreting these features, we suggest a procedure that in some experimental situations may be useful to distinguish generally-shaped cracks from volume defects and to determine for elliptically-shaped cracks the orientation, shape and size.

[*]Author to whom all correspondence should be sent. Phone: (505) 667-6727.

CRACK IDENTIFICATION AND CHARACTERIZATION
IN LONG WAVELENGTH ELASTIC WAVE SCATTERING

INTRODUCTION

Cracks can cause significant changes in the mechanical behavior of materials, the most dramatic change being the possibility of fracture. Nondestructive detection of cracks, especially cracks critical to fracture, often utilizes ultrasonic techniques in which an elastic wave propagates through the material and is scattered by the crack. From features of the scattering, the detection and characterization of the crack is attempted. Clearly, in these important experiments the dominant physical process to be understood is the scattering of the elastic wave by a particular crack. In this respect, a simple model predicts that an elliptical or circular "soft" crack embedded in a uniform, isotropic medium.

Recently, several investigators[1-5] independently considered the scattering from cracks of this problem in the limiting case where the wavelength of the elastic wave is considerably larger than the crack. In this parametric Rayleigh limit, the exact form of the scattering amplitude can be obtained.

In this paper we imitate the spirit, but extend the analysis, of these investigations. Our approach is to start with a volume integral formulation of the scattering[8,9] for which several useful approximations exist.[9-12] The approximation used here is identical to the quasi-static result derived by Datta.[3] Our purpose is to illustrate in the context of this approximation

apparent characteristic features of elastic wave scattering from cracks, to interpret these results and to discuss experimental procedures that may be useful for their detection and characterization.

More explicitly, we first identify scattering signatures which distinguish cracks of general shape from volume defects (voids and inclusions). Then, we specialize our study to elliptical cracks and propose scattering signatures which allow the determination of the crack orientation, size and shape. Also the applicability of measuring these signatures in realistic non-destructive testing situations is assessed.

BASIC EQUATIONS

The basic scattering picture is depicted in Fig. 1. An arbitrarily shaped cavity with a surface ∂ bounding a region R is embedded in an infinite, homogeneous, elastically isotropic medium. The incident power is directed along the positive z-axis and is monochromatic with an angular frequency . The unit vector $\hat{r}$ determines the direction of observation of the scattered power relative to some suitably chosen Cartesian coordinate system.

The scattering effectiveness of this cavity is measured by the differential cross-section which is essentially the time average of the fraction of incident power scattered into a particular direction. For incident power associated with a displacement field [omitting $\exp(-i\omega t)$]

$$u_i^0 = a_i e^{i\underline{\alpha}^0 \cdot \underline{r}} + b_i e^{i\underline{\beta}^0 \cdot \underline{r}} \tag{1}$$

where α and β are the wavenumbers of the longitudinal and transverse made with a_i and b_i, the corresponding vector polarization amplitudes, and $\underline{\alpha}^0 = \lambda\underline{\hat{a}}$ and $\underline{\beta}^0 = \beta\underline{\hat{a}}$, the incident wavevectors. The differential cross-section is found[8] to be given by

$$\frac{dP(\omega)}{d\Omega} = \frac{\alpha(\lambda+2\mu)|A_i|^2 + 2\mu|B_i|^2}{\alpha(\lambda+2\mu)|a_i|^2 + 2\mu|b_i|^2} \tag{2}$$

with λ and μ the Lamé parameters of the medium hosting the cavity, $d\Omega$ a differential element of solid angle, and A_i and B_i the vector amplitudes of the displacement field associated with the scattered (far-field) power:

$$u_i^0 \sim A_i \frac{e^{i\alpha r}}{r} + B_i \frac{e^{i\beta r}}{r} \tag{3}$$

The scattered amplitudes are related to a quantity called the f-vector[8]

$$A_i = \hat{r}_i \hat{r}_j f_j(\underline{\alpha}) \tag{4a}$$

and

$$B_i = (\delta_{ij} - \hat{r}_i \hat{r}_j) f_j(\underline{\beta}) \tag{4b}$$

where summation over repeated indices is implied (as throughout the rest of the paper), $\underline{\hat{r}}$ is the unit vector in the scattered (observation) direction, and $\underline{\alpha} = \alpha\underline{\hat{r}}$ and $\underline{\beta} = \beta\underline{\hat{r}}$. For a void the the explicit form of the f-vector is

$$f_i(\underline{k}) = \frac{-k^2}{4\pi\rho\omega^2}\left[\rho\omega^2 \int_R dVu_i e^{-i\underline{k}\cdot\underline{r}} + ikC_{ijk\ell}\hat{r}_j \int_R dV\epsilon_{k\ell}e^{-i\underline{k}\cdot\underline{r}}\right] \quad (5)$$

where $C_{ijk\ell} = \lambda\delta_{ij}\delta_{k\ell} + \mu(\delta_{i\ell}\delta_{jk} + \delta_{ik}\delta_{j\ell})$.

One of our objectives is to apply Eq. (5) to the long wave scattering from a crack. To indicate the nature of our approximation, we write

$$f_i(\underline{k}) \equiv f_i\left[u_i e^{-i\underline{k}\cdot\underline{r}} ; \quad \epsilon_{k\ell}e^{-i\underline{k}\cdot\underline{r}}\right] \quad (6)$$

to symbolize that in (5) there are two independent integrations, one with $u_i \exp(-i\underline{k}\cdot\underline{r})$ in the integrand and the other with $\epsilon_{k\ell}\exp(-i\underline{k}\cdot\underline{r})$; that is,

$$f_i[x_i; y_k] = \frac{k^2}{4\pi\rho\omega^2}\left[\ldots^2 \int_R dVx_i + ikC_{ijk\ell}\hat{r}_j \int_R dVy_{k\ell}\right] . \quad (7)$$

A specific choice of these fields will produce the exact $f_i(\underline{k})$. Our approximation is based on substituting known fields for x_i and $y_{k\ell}$, and as choices for these fields, we consider first a **static** problem of a cavity embedded in a medium that has a uniform stress σ_{ij}^0 as $R \to \infty$. The resulting strain field can be written as

$$\epsilon_{ij}^\sigma = e_{ij}^0 + \int_R dVG_{ijk\ell}^{(s)}C_{k\ell mn}\dot{\epsilon}_{mn} \quad (8)$$

where e_{ij}^0 is the strain field associated with σ_{ij} in the defect-free medium, $G_{ijk\ell}^{(s)}$ is the static Green's function[13,14] and $\dot{\epsilon}_{ij}$ is a fictitious field defined in the cavity. For ellipsoidal cavities $\dot{\epsilon}_{ij}$ was calculated by Eshelby.[7] It is exactly the static field used in approximate solution. Returning now to the scattering

problem, we note that for an incident wave of the form

$$u_i^0 = u_i^\sigma e^{i\underline{k}^0 \cdot \underline{r}}$$ (9)

the associated strain field is

$$\varepsilon_{ij}^0 = e_{ij}^0 e^{i\underline{k}^0 \cdot \underline{r}}$$

where

$$e_{ij}^0 = i\left(u_i^\sigma k_j^0 + u_k^\sigma k_i^0\right)/2 \quad .$$ (10)

With e_{ij}^0 as a static, uniform strain, the tensor ε_{ij}^σ (associated with the corresponding static problem) is defined. When f_i^{QS} is used in Eq. (4), the approximation

$$f_i^{QS} = f_i\left[u_i^\sigma ; \varepsilon_{k\ell}^\sigma\right]$$ (11)

can be shown[3,11,12] to produce the scattered amplitudes exactly to the leading order in ω (which is ω^2). Equation (10) is called the quasi-static approximation[11]; it gives the Rayleigh limit to the scattering.

For ellipsoidal cavities, the ε_{ij}^σ needed in Eqs. (8) and (11) is given by Eshelby; furthermore, ε_{ij}^σ is itself a uniform (constant) strain. For an ellipsoid, Eq. (5) becomes

$$f_i^{QS}(\underline{k}) = \frac{-Vk^2}{4\pi\rho\omega^2}\left[\rho\omega^2 u_i^\gamma + ikC_{ijk\ell}\hat{r}_j\varepsilon_{k\ell}^\sigma\right]$$ (12)

where V is the volume of the cavity. ε_{ij}^σ is related to e_{ij}^0 by

$$\varepsilon_{ij}^\sigma = [(I-S)^{-1}]_{ijk\ell}\, e_{k\ell}^0 \equiv \Gamma_{ijk\ell}\, e_{k\ell}^0$$

where I is the identity fourth rank tensor and the fourth rank tensor S is calculated by Eshelby.[7]

To obtain results for an elliptical crack, we first consider an ellipsoid with principal axes $a > b > c$, and then take the following limits:

$$\lim_{c \to 0} V = 0$$

$$\lim_{c \to 0} V\Gamma_{ijk\ell} \equiv \gamma_{ijk\ell}$$

More explicitly, if a and b are along the x- and y-directions, we find

$$\gamma_{3311} = \gamma_{3322} = \frac{4\pi a^3}{3} \frac{2\nu(1-\nu)\kappa_1^2}{E(\kappa)(1-2\nu)} \tag{13a}$$

$$\gamma_{3333} = \frac{1-\nu}{\nu} \gamma_{3311} \tag{13b}$$

$$\gamma_{2323} = \frac{2\pi a^3 \kappa_1^2}{3}\left[\frac{E(\kappa)}{1-\nu} - \frac{\nu\kappa_1^2[F(\kappa)-E(\kappa)]}{\kappa^2(1-\nu)}\right]^{-1} \tag{13c}$$

$$\gamma_{1313} = \frac{2\pi a^3 \kappa_1^2}{3}\left[E(\kappa) + \frac{\nu\kappa_1^2[F(\kappa)-E(\kappa)]}{\kappa^2(1-\nu)}\right]^{-1} \tag{13d}$$

where ν is Poisson's ratio $[\nu=\lambda/2(\lambda+\mu)]$ and $F(\kappa)$ and $E(\kappa)$ are complete elliptic integrals of the first and second kind with $\kappa = (1 - b^2/a^2)^{1/2}$ and $\kappa_1^2 = 1 - \kappa^2$. The corresponding expressions for a circular crack of radius a are

$$\gamma_{3311} = \gamma_{3322} = \frac{16a^3}{3} \frac{\nu(1-\nu)}{1-2\nu} \tag{14a}$$

$$\gamma_{3333} = \frac{(1-\nu)}{\nu} \gamma_{3311} \tag{14b}$$

$$\gamma_{2323} = \gamma_{1313} = \frac{8a^3}{3} \frac{(1-\nu)}{(2-\nu)} . \tag{14c}$$

For both elliptical and circular cracks $\gamma_{ijk\ell} = \gamma_{jik\ell} = \gamma_{ij\ell k}$. Terms that cannot be obtained from (13) by these interchanges of indices are zero. We note that $\gamma_{ijk\ell}$, and hence the scattered

fields, are proportional to $4\pi a^3/3$, the volume of the smallest sphere that can encircle the crack independent of b. We note that

$$\gamma_{3311}/\gamma_{1313} + \gamma_{3311}/\gamma_{2323} = 2(2 - \nu)/(1 - 2\nu) \qquad (15)$$

and hence that only two of the $\gamma_{ijk\ell}$ are independent.

RESULTS

In this section we address the problem of flaw characterization in two stages. First, several features are found that distinguish cracks from volume defects, including one valid for arbitrarily-shaped (not necessarily planar) cracks. Second, for the special case of elliptical cracks, we discuss procedures for determining crack orientation, size and shape. The applicability of these procedures to realistic non-destructive testing situations is also assessed.

Crack Identification

In the quasi-static limit the f-vector for scattering from a cavity has form[1]

$$f_i = VPu_i^\sigma + Q_{ij}\hat{r}_j \qquad (16)$$

where

$$P = -k^2/4\pi \qquad (17a)$$

and

$$Q_{ij} = \frac{-ik^3}{4\pi\rho\omega^2} C_{ijk\ell} \int_R d\underline{r}\ \varepsilon_{k\ell}^\sigma(\underline{r}) \qquad (17b)$$

Alternately, Q_{ij} can be obtained using the surface integral formulation of the problem. With a crack regarded as the limiting case of the volume $V \to 0$,

$$f_i = Q_{ij}^* \hat{r}_j$$

with

$$Q_{ij}^* = \lim_{V \to 0} Q_{ij}$$

But as seen from (17b) the tensor Q_{ij}, and hence Q_{ij}^*, depends only on the incident field and <u>not</u> on the scattered direction $\hat{r}$. Thus, from (4a) the magnitude of the longitudinal field is

$$A_i \hat{r}_i = f_i \hat{r}_i = Q_{ij}^* \hat{r}_i \hat{r}_j$$

which is invariant under the replacement of $\hat{\underline{r}}$ by $-\hat{\underline{r}}$. Physically, for any incident direction this means the scattering in any two diametrically opposite directions is identical (Fig. 2). This general result is valid only for cracks since the first term in (16) is nonzero for all cavities (and more generally for all inclusions). Consequently, if the measured scattered fields are equal at any two diametrically opposite points, the defect must be a crack. A similar analysis can be made for the amplitude of the transverse scattered fields with the identical conclusion.

Considering the special case of elliptical cracks, we can find other scattering signatures of cracks. Below we give for an incident longitudinal plane wave the Rayleigh limit scattered amplitudes and explicitly illustrate these signatures. In our equations, $\gamma^{(0)} = \gamma_{3311}$, $\gamma^{(1)} = \gamma_{1313}$ and $\gamma^{(2)} = \gamma_{2323}$; the incident direction $\hat{\underline{a}}$ is characterized by the angles ζ_0 and ϕ_0; and the scattered direction $\hat{\underline{r}}$, by θ and ϕ. All angles are defined in a coordinate system fixed by the principal axes of the crack and by $\hat{\underline{n}}$, and the semi-major axis a and semi-minor axis b are in the x- and y- directions while $\hat{\underline{n}}$ is in the z-direction (Fig. 3).

For a longitudinal wave incident in an arbitrary direction,

$$\underline{u}^\sigma = \cos \phi_0 \sin \theta_0 \hat{\underline{x}} + \sin \phi_0 \sin \theta_0 \hat{\underline{y}} + \cos \theta_0 \hat{\underline{z}}$$

and

$$\underline{a}^\bullet = \alpha \, \hat{\underline{u}}^\sigma \ ,$$

the scattered longitudinal (L) and transverse (T) displacement fields are

$$A_i = \hat{r}_i \frac{\alpha^2}{4\pi} \frac{\nu}{1-\nu} \left\{ \gamma^{(0)} \left[1 + \frac{(1-2\nu)}{\nu} \cos^2 \theta \right] \right. \tag{18a}$$

$$\times \left[1 + \frac{(1-2\nu)}{\nu} \cos^2 \theta_0 \right] + \frac{(1-2\nu)}{2\nu} \left[\gamma^{(1)} \cos \phi \cos \phi_0 \right.$$

$$\left. + \gamma^{(2)} \sin \phi \sin \phi_0 \right] \sin 2\theta \sin 2\theta_0 \bigg\}$$

$$B_i = \frac{\alpha\beta}{4\pi} \left(\hat{\theta}_i \left\{ -\gamma^{(0)} \left[1 + \frac{(1-2\nu)}{\nu} \cos^2 \theta_0 \right] \sin 2\theta \right. \right. \tag{18b}$$

$$+ \sin 2\theta_0 \cos 2\theta \left[\gamma^{(1)} \cos \phi \cos \phi_0 + \gamma^{(2)} \sin \phi \sin \phi_0 \right] \bigg\}$$

$$\left. - \hat{\phi}_i \sin 2\theta_0 \cos \theta \left[\gamma^{(1)} \sin \phi \cos \phi_0 - \gamma^{(2)} \cos \phi \sin \phi_0 \right] \right)$$

where $\hat{\underline{\theta}}$ and $\hat{\underline{\phi}}$ are unit vectors in the θ and ϕ directions. By inspecting these equations, we found 3 additional crack identi- fiers: One, if both the incident and scattered directions are anywhere in the crack plane ($\theta = \theta_c = 90°$), then the magnitudes of the scattered fields, and hence the cross-sections, are constants:

$$A = \alpha^2 \nu \gamma^{(0)} / 4\pi (1-\nu) \tag{19a}$$

$$B = 0 \tag{19b}$$

Thus, the plane of the crack is a "plane of constant scattering". Furthermore, the existence of such a plane is a special property of elliptical cracks and is useful not only to distinguish these from volume defects, but also to determine the crack plane orienta- tion, $\hat{\underline{n}}$. (See below.)

Two, for normal incidence and for incidence along the crack edge ($\zeta_0 = 0°$ and $90°$), the angular distribution of scattered L waves (and similarly for scattered T waves) is identical and also independent of ζ_0 and ζ, that is,

$$A = 1 + \frac{(1-2\nu)}{\nu} \cos^2 \zeta \tag{20a}$$

$$B = |\sin 2\zeta| \tag{20b}$$

Three, as seen from (20), the scattering for normal incidence is twofold symmetry about $\cdot = 90°$ (i.e. the crack plane). This feature is also absent in the scattering from volume defects. [From (4) and (12) it can be demonstrated that the contribution gives rise to an additional cos · dependence for L waves and a $\sin \theta$ dependence for T waves.]

Thus, to leading order in .., the scattered power has a higher symmetry than the scatterer; furthermore, there are simple, measurable, qualitative features of the scattering that not only distinguish an elliptical crack from volume defects, but also determine the crack plane orientation.

Crack Characterization

Maintaining our specialization to elliptical cracks, we now discuss features that characterize the cracks. This characterization consists of the determination of the orientation, size and shape.

Our first task is to determine the orientation of the crack plane. For elliptical cracks this task can be accomplished concurrently with the task of differentiating cracks from elliptical defects. For example, the plane of constant scattering is coincident with the crack plane.

The more difficult task is to determine the orientation within this plane of the crack major axis. Knowing the crack plane allows us to specify and ζ_3 in (16). To complete the specification of the crack orientation one must utilize the ϕ-dependence of the scattering. By inspecting (19) one sees that the relative magnitude of the ϕ-dependent terms is maximized when $\theta = \zeta_0 = 45°$. In that case, for a pulse-echo experiment $(\zeta = \zeta_3)$, the scattered longitudinal amplitude is, for example,

$$A_1 \hat{P}_1 = p + q \cos^2 \phi \qquad (21a)$$

where

$$p \qquad \frac{\alpha^2}{16\pi(1-\nu)} \left[2 \gamma^{(0)} + (1 - 2\nu) \gamma^{(2)} \right] \qquad (21b)$$

$$q = \frac{\alpha^2}{16\pi(1-\nu)} \quad (1-2\nu)[\gamma^{(1)} - \gamma^{(2)}] \qquad (21c)$$

Since $p, q < 0$, the maxima of the backscattered power (at $\phi = 0°$ or $180°$) locate the direction of the major axis. However, the ϕ dependence is proportional to $\gamma^{(1)} - \gamma^{(2)}$, which (Fig. 4) may be too small to measure for all b/a ratios. Consequently, the orientation of the major axis may be hard to determine experimentally. Physically, in the Rayleigh limit, scattering by an elliptical crack is similar to scattering by a circular crack.

This discussion bears directly on the last task characterizing the crack, the determination of a and b/a. In principle, knowledge of any two of $[\gamma^{(0)}, \gamma^{(1)}, \gamma^{(2)}]$ is sufficient to uniquely determine a and b/a. However, Figs. 4 and 5 reveal that $\gamma^{(1)} - \gamma^{(2)}$ and $p/(p+q)$, the ratio of the minimum to maximum value of (21a), depend very weakly on b/a;

as such, experimental determination of ... may be difficult.

For example, from Fig. ..., the value of ...

by exact measurement of ... . Then, with Fig. ..., ...

of $\gamma^{(0)}$ determines ... . However, from ... ...

variation from ... (needle ... ...

crack) results ... . Thus, it

seems that the ... limit can ...

determ... ...

can, then, ...

tion concern... the surf... ...

$x_2 = b$ ... and ...

meas...

$$[\gamma^{(0)}, \ldots] \qquad (22)$$

where ...

A sin... ...

incid... ...

CONCLUSIONS

In contrast to long wavelength scattering of acoustic or quantum mechanical waves, which are isotropic with little information about the scatterer, the scattering of elastic waves, in addition to an isotropic component, possesses dipolar and quadrapolar components with important information about the scatterer.[1] We examined the angular content for the scattering from cracks and, after examining this content, identified features that may be useful in crack characterization experiments.

With great generality, we found that for any angle of incidence the Rayleigh scattering from any crack, in contrast to the scattering from volume defects, is identical in any two diametrically opposite directions. This feature identifies the defect as a crack, but does not characterize the crack as to its size, shape and orientation. Additional identifying features, as well as a characterizing procedure, were specified for an elliptical crack. In this case, we found that it is in principle possible to characterize the crack uniquely. In practice, because of certain shape insensitive parameters, we believe the crack may appear circular, and probably the best one can do is to measure the crack plane orientation and bounds for the crack length a.

ACKNOWLEDGEMENTS

REFERENCES

1. Gubernatis, J. E., J. A. Krumhansl and R. M. Thomson, "Interpretation of Elastic Wave Scattering Theory for Analysis and Design of Flaw Characterization Experiments: The Long Wavelength Limit", Los Alamos Scientific Laboratory Report LA-UR-78-784, submitted to J. Appl. Phys.

2. Domany, E., J. A. Krumhansl and S. Teitel, "Quasistatic Approximation to the Scattering of Elastic Waves by a Circular Crack", J. Appl. Phys. 49 (1977): 2599.

3. Datta, S. K., "Diffraction of Plane Elastic Waves by Ellipsoidal Inclusions", J. Acoust. Soc. Am. 61 (1977): 1432.

4. Kohn, W., and J. R. Rice, "Scattering of Long Wavelength Elastic Waves from Localized Defects in Solids", submitted to J. Appl. Phys.

5. Budiansky, B. and J. R. Rice, "On the Estimation of a Crack Fracture Parameter by Long Wavelength Scattering", unpublished.

6. Kraut, E. A., "Review of Theories of Scattering of Elastic Waves by Cracks", IEEE Trans. Sonics Ultrason. 23 (1976): 162.

7. Eshelby, J. D., "The Determination of the Elastic Field of an Ellipsoidal Inclusion and Related Problems", Proc. Roy. Soc. London 271 (1957): 376.

8. Gubernatis, J. E., E. Domany and J. A. Krumhansl, "Formal Aspects of the Theory of the Scattering of Ultrasound by Flaws in Materials", J. Appl. Phys. 48 (1977): 2804.

9. Gubernatis, J. E., E. Domany, J. A. Krumhansl and M. Huberman, "Theory of the Scattering of Ultrasound by Flaws", in 1975 Ultrasonics Symposium Proceedings, ed. by J. de Klerk. New York, IEEE, 1975, p. 107.

10. Gubernatis, J. E., E. Domany, M. Huberman, and J. A. Krumhansl, "The Fundamental Theory of Elastic Wave Scattering by Defects in Elastic Materials: Integral Equation Methods for Application to Ultrasonic Flaw Detection", Materials Science Center Report 2654, Cornell University, 1975.

11. Gubernatis, J. E., "Long Wave Approximations for the Scattering of Elastic Waves from Flaws", Los Alamos Scientific Laboratory Report LA-UR-77-2900, submitted to J. Appl. Phys.

12. Gubernatis, J. E., "The Scattering of Long Wavelength Elastic Waves from Ellipsoidal Voids and Inclusions", unpublished.

13. Gubernatis, J. E., E. Domany and J. A. Krumhansl, "The Elasticity of Polycrystals and Rocks", J. Geo. Res. 80 (1975): 4851.

14. Gubernatis, J. E. and E. Domany, "Macroscopic Engineering Properties of Polycrystalline Materials: Elastic Properties", J. Appl. Phys. 46 (1975): 1875.

15. Gubernatis, J. E. and E. Domany, "Rayleigh Scattering of Elastic Waves from Cracks", unpublished.

FIGURE CAPTIONS

Fig. 1   A typical scattering geometry. For purposes of illustration the incident power is along the positive z-axis.

Fig. 2   The coordinate system defining the incident angles ℓ_0 and ς_0 and the scattered angles ℓ and ς relative to the crack orientation.

Fig. 3   An invariance property of Rayleigh scattering from cracks. For an incident direction $\hat{\underline{a}}$ the scattering in the direction $\hat{\underline{r}}$ is equal to the scattering in the direction $-\hat{\underline{r}}$.

Fig. 4   Curves of $\gamma^{(0)}$, $\gamma^{(1)}$ and $\gamma^{(2)}$ as a function of b/a. The $\gamma^{(0)}$, $\gamma^{(1)}$ and $\gamma^{(2)}$ have units of volume with the unit of length the same as a and b. $\nu = \frac{1}{4}$.

Fig. 5   A measure of the sensitivity of the scattering from an elliptical crack to its shape, b/a. $\nu = \frac{1}{4}$.
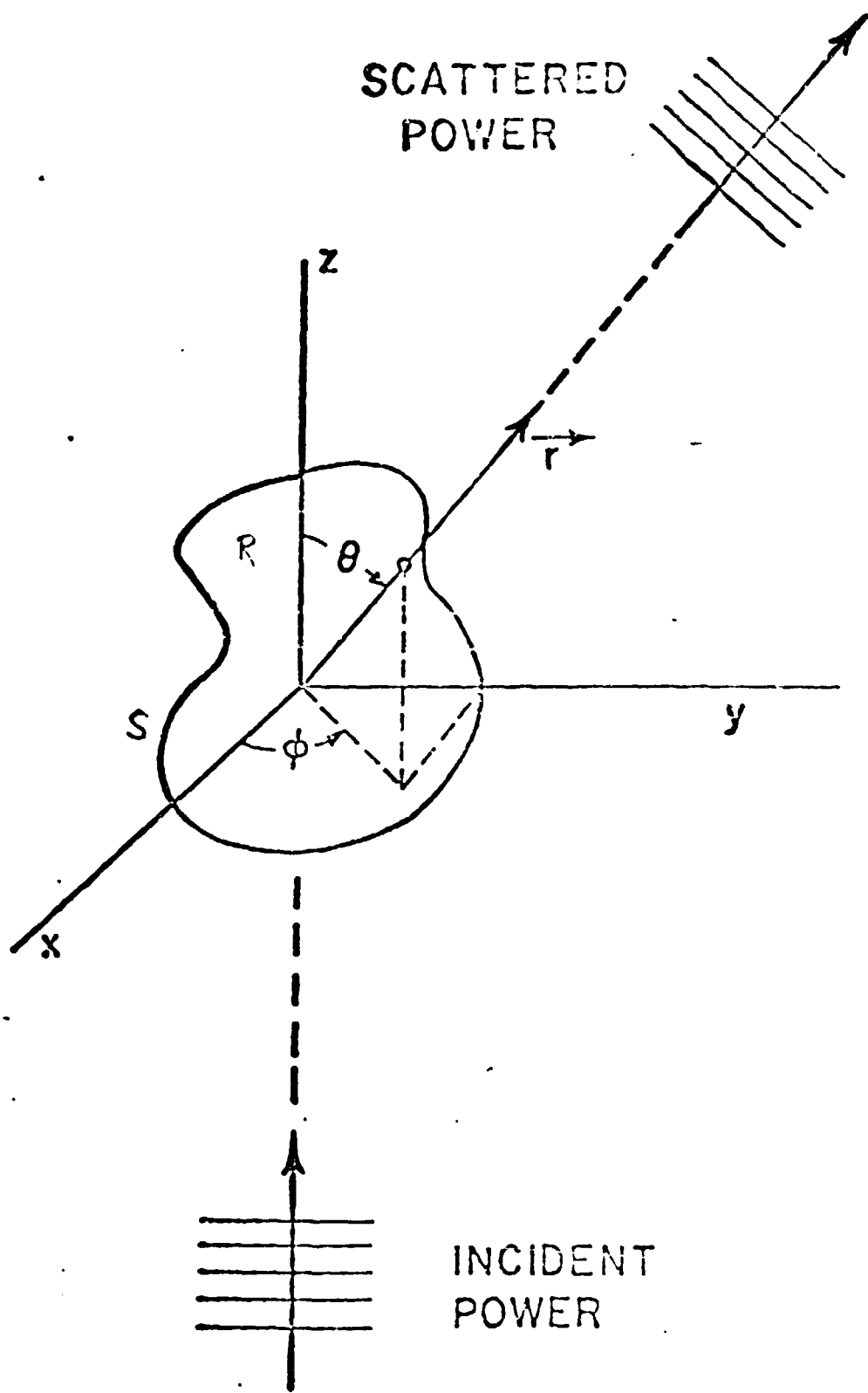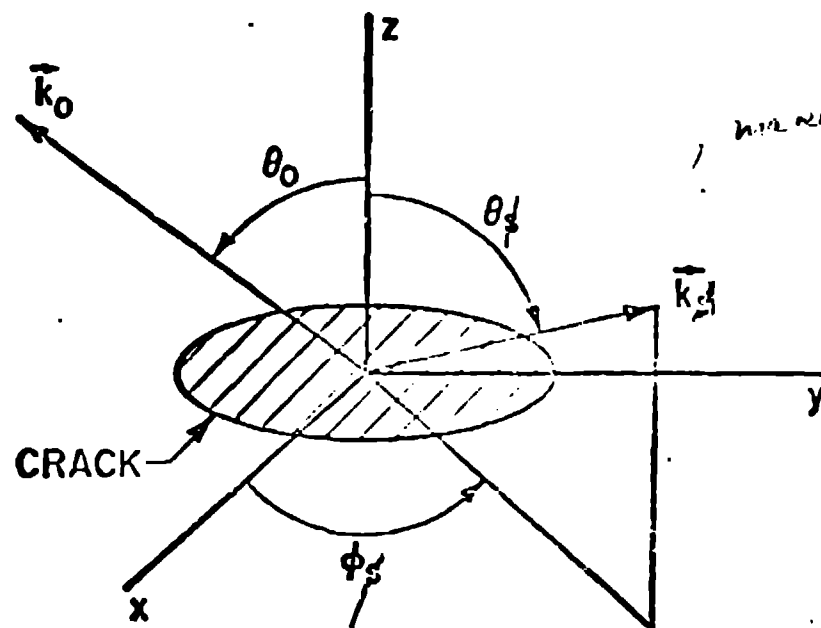
SCATTERED POWER

z

R

θ

$\vec{r}$

S

φ

y

x

INCIDENT POWER

Fig. 1

Fig. 2

Fig. 3

Fig. 4

Fig. 5